MAUSAM, **72**, 1 (January 2021), 57-76

551.515.2 : 551.509 (267)

A review of the development and implementation of a tropical cyclone prediction system for North Indian Ocean in a multi-model ensemble framework

S. SARANYA GANESH*, **, S. ABHILASH*, ***, S. JOSEPH, MANPREET KAUR*, **, A. DEY*, R. MANDAL*, R. PHANI*, R. CHATTOPADHYAY*, D. R. PATTANAIK**** and A. K. SAHAI*, #

**Indian Institute of Tropical Meteorology, MoES, Dr. Homi Bhabha Road, Pashan, Pune – 411 008, India*

***Department of Atmospheric and Space Sciences, Savitribai Phule Pune University, Pune – 411 007, India*

****Department of Atmospheric Sciences, Cochin University of Science and Technology, Cochin – 682 022, India*

*****India Meteorological Department, Ministry of Earth Sciences, New Delhi – 110 003, India*

#e mail : sahai@tropmet.res.in

सार – डब्लू. एम. ग्रे द्वारा विकसित उष्णकटिबंधीय चक्रवात जनन के लिए ऋतुनिष्ठ प्राचलों का व्यापक रूप से उपयोग उष्णकटिबंधीय महासागरों में बनने वाले चक्रवातों के जलवायविक और ऋतुनिष्ठ निगरानी के लिए किया जाता है। उत्तर हिंद महासागर (NIO) पर, भारत मौसम विज्ञान विभाग द्वारा अलग-अलग नियतात्मक और संभावित पूर्वानुमान तकनीकों के कार्यान्वयन के साथ चक्रवात बनने और उसके आगे बढ़ने की निगरानी तथा लघु, मध्य एवं विस्तारित अवधि का पूर्वानुमान दिया जाता है। इस शोध पत्र में उष्णकटिबंधीय चक्रवात के पूर्वानुमान के लिए इन-हाउस विकसित की गई प्रणाली की समीक्षा की गई है जो बेहतर तूफान विकास सूचकांक और चक्रवात बनने,आगे बढ़ने तथा मार्ग का पता लगाने के लिए एक ट्रैकिंग एल्गोरिथ्म है । इसे बाद में संसाधित मल्टी मॉडल एन्सेम्बल (MME) से जलवायु पूर्वानुमान प्रणाली आधारित ग्रैंड एन्सेम्बल प्रेडिक्शन सिस्टम (CGEPS) से प्रचालनात्मक विस्तारित अवधि पूर्वानुमान देने के लिए लागू किया गया।

इसके पहले भाग में, एक से अधिक तूफान प्रणालियों के एक साथ विकसित होने पर चक्रवात बनने के पूर्वानुमान देने की विश्वसनीयता एक केस स्टडी का उपयोग करके की जाती है। प्रमुख चक्रवात जनन सूचकांकों और इसके घटक प्राचलों का उपयोग वायुमंडलीय और महासागरीय विशेषताओं का विश्लेषण करने के लिए किया जाता है, जिन्होंने ERA -अंतरिम दैनिक औसत डेटासेट का उपयोग करके उत्तरी हिंद महासागर पर लगातार दो तूफानों को प्रभावित किया। MME आउटपुट से सूचकांकों के प्रदर्शन का विश्लेषण भी किया जाता है। इसके अलावा ERA-5 और ERA-अंतरिम डेटासेट का उपयोग करके मार्ग पूर्वानुमान प्रणाली की विश्वसनीयता पर चर्चा की जाती है। अंत में, हाल ही में आए उष्णकटिबंधीय चक्रवातों अम्फन और निसर्ग का पूर्वानुमान देने में CGEPS- MME के प्रदर्शन पर विस्तार से चर्चा की गई है। इस पूर्वानुमान प्रणाली के वास्तविक समय में क्रियान्वयन से तूफानों के बनने पर आरंभिक मार्गदर्शन प्रदान करने में महत्वपूर्ण सहायता मिली है, जिससे चक्रवात चेतावनी समुदाय को अलर्ट पर रखा जा सके, और बेहतर नियोजन एवं शमन कार्यों के लिए पर्याप्त समय मिल सके।

ABSTRACT. The seasonal genesis parameters for tropical cyclogenesis developed by W. M. Gray, is widely used for the climatological and seasonal monitoring of cyclogenesis over the tropical oceans. Over the North Indian Ocean (NIO), cyclogenesis and evolution is monitored and predicted in the short, medium and extended ranges by India Meteorological Department with the implementation of different deterministic and probabilistic forecasting techniques. This paper provides a review of an in-house developed tropical cyclone prediction system involving an improved storm evolution index and an objective tracking algorithm for detecting cyclogenesis, evolution and storm tracks from post-processed Multi-model ensemble (MME) outputs from the Climate Forecast System-based Grand Ensemble Prediction System (CGEPS) implemented for operational extended range prediction.

In the first part, the reliability of cyclogenesis prediction when more than one storm systems develop simultaneously is discussed using a case study. Prominent cyclogenesis indices and constituent parameters are used to analyse the atmospheric and oceanic features which affected the evolution two consecutive storms over NIO by using ERA-Interim daily averaged datasets. The performance of indices from MME outputs is also analysed. Further the reliability of objective track prediction system is discussed by using ERA-5 and ERA-Interim datasets. Finally, the performance of the CGEPS-MME in predicting the recent tropical cyclones, Amphan and Nisarga are discussed in detail. Real-time implementation of this prediction system has proven to be critical in providing early guidance on the formation

of storms, enabling the cyclone warning community to be on alert thereby providing enough lead time for better planning and mitigation strategies.

Key words – North Indian Ocean cyclogenesis, Tropical cyclone prediction system, Cyclogenesis potential parameter, Objective tracking algorithm, Multi-model ensemble prediction system.

1. Introduction

Tropical storms that develop over Northern Indian Ocean basin (NIO) comprising of Arabian Sea (AS) and Bay of Bengal (BoB) pose a major threat to the vast peninsular Indian coasts teeming with cities having excess population and high rises as well as large areas of low-lying agricultural plantations. With each year, the economic and property losses due to storm-induced gales, landslides and flash floods over the affected regions is becoming more severe. Over NIO, the intense cyclonic activity occurs primarily, unlike other ocean basins, in the monsoon transitional seasons of spring and autumn since monsoon trough will be located mostly over the open waters of NIO and due to the occurrences of weak vertical wind shear that provide favourable conditions for cyclogenesis (Lee *et al.*, 1989). These are the pre-monsoon (April to June) and post-monsoon (October to December) periods (Fig. 1) with frequency of genesis over BoB higher than AS. 75% of the storms develop over BoB basin as AS is relatively colder than BoB and hence inhibits the formation and intensification of storms (Gray, 1979). The decrease in easterly shear due to weakening of Tropical Easterly Jet (TEJ) has resulted in increased cyclogenesis of severe tropical cyclones and reduction in number of depressions during the onset and retreat periods of Indian summer monsoon. An early decrease in the shear of easterly jet is due to higher warming or due to reduction in the temperature gradient in the tropical belt (Krishna, 2009).

Extensive research in the field of genesis and evolution of Tropical Cyclones is done by the W. M. Gray, publishing a series of articles on cyclogenesis of different ocean basins (Gray, 1968, 1975, 1979, 1984, 1998) leading to six necessary climatological genesis parameters for tropical cyclogenesis constituting of three dynamical and thermodynamic variables each. They are: (*i*) high values of low-level relative vorticity, (*ii*) low values of vertical wind shear, (*iii*) enough Coriolis force required to initiate circulation around the low pressure centre, (*iv*) high values of Sea Surface Temperature (SST) exceeding 26 °C with a deep thermocline, (*v*) ample mid-tropospheric moisture and (*vi*) highly unstable atmosphere. Inspired by Gray's parameters, numerous studies emerged defining cyclogenesis indices for different ocean basins (McBride and Zehr, 1981; Zehr *et al*., 1992; DeMaria *et al.*, 2001; Emanuel and Nolan, 2004; Kotal *et al.*, 2009; Ganesh *et al.*, 2020). Out of these, a widely acclaimed seasonal parameter, Genesis Potential Index (GPI) developed by Emanuel and Nolan (2004) include a set of chosen predictors; maximum potential intensity (Emanuel, 1986), relative humidity, absolute vorticity at various levels and vertical wind shear.

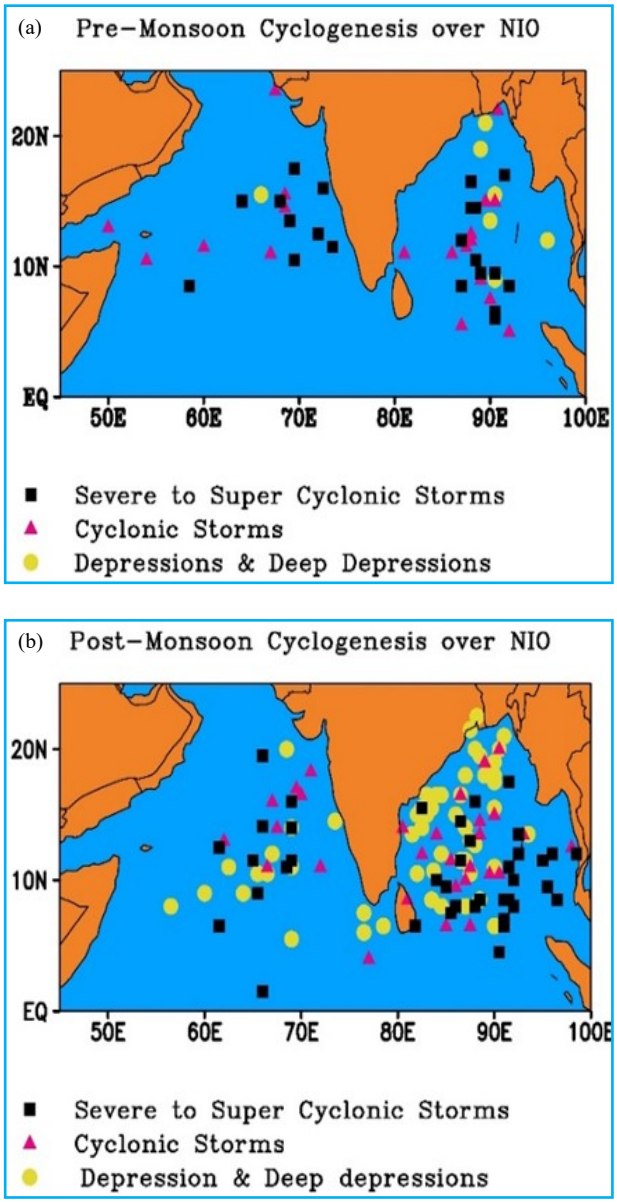

Figs. 1(a&b). Observed cyclogenesis locations from IMD-Best Track datasets over NIO during (a) Pre-monsoon and (b) Post-monsoon periods from 1991-2017

TABLE 1

List of selected storm cases

S. No.	Cyclone Name	Season Pre-monsoon / Post-monsoon	Basin (AS / BoB)	Date of formation (DDMMYYYY)	Life-time Days	Storm Category (IMD, 2016)	Observed Genesis Positions (Lat. °N / Long. °E)
1.	Nisarga	Pre-monsoon	AS	01 Jun, 2020	4	SCS	13 N / 71.4 E
2.	Amphan	Pre-monsoon	BoB	16 May, 2020	6	SuCS	10.4 N/ 87 E
3.	Ockhi	Post-monsoon	AS	29 Nov, 2017	6	VSCS	6.5 N/ 81.8 E
4.	Deep Depression 2017	Post-monsoon	BoB	05 Dec, 2017	5	DD	8.5 N/ 88.5 E
5.	Ashobaa	Pre-monsoon	AS	07 Jun, 2015	6	CS	14.5 N / 68.5 E
6.	Chapala	Post-monsoon	AS	28 Oct, 2015	8	ESCS	11.5 N / 65 E
7.	Nanauk	Pre-monsoon	AS	10 Jun, 2014	5	CS	15.5 N / 68.5 E
8.	Nilofar	Post-monsoon	AS	25 Oct, 2014	7	ESCS	12.5 N / 61.5 E
9.	Megh	Post-monsoon	AS	05 Nov, 2015	6	ESCS	14.1 N / 66 E
10.	Phailin	Post-monsoon	BoB	08 Oct, 2013	7	ESCS	12 N / 96 E
11.	Viyaru	Pre-monsoon	BoB	11 May, 2013	6	CS	5 N / 92 E
12.	Lehar	Post-monsoon	BoB	23 Nov, 2013	6	VSCS	8.5 N / 96.5 E
13.	Hudhud	Post-monsoon	BoB	07 Oct, 2014	7	ESCS	11.5 N / 95 E
14.	Helen	Post-monsoon	BoB	19 Nov, 2013	4	SCS	14.5 N / 86.5 E

GPI generally show very good skill in capturing genesis frequencies in inter-annual time scales over the northwest Pacific and north Atlantic regions compared to NIO (Camargo *et al.*, 2007). During pre-monsoon and post-monsoon periods, middle-tropospheric humidity and lower-level vorticity alone do not provide the essential cyclogenesis. Genesis potential is high due to reduced vertical shear in wind and maximum potential intensity. Unlike other basins, the cyclogenesis inducing weather noises over NIO basin are less compared to other basins mainly due to the unique geological position of the peninsula as well as warm sea surface temperatures. A larger GPI may not always mean higher chances of cyclogenesis due to insufficient weather noise asthe major cyclogenesis inducing factors over NIO are the intra-seasonal oscillations; Boreal Season Intra-Seasonal Oscillations & Madden Julian Oscillations that provide lower level circulation and ample moisture in the middle-troposphere enabling cyclogenesis over favourable warm oceans and low vertical wind shear. (Kikuchi & Wang, 2010; Krishnamohan *et al.*, 2012). The pre-monsoon and post-monsoon are the major cyclone seasons as the vertical wind shear will be favouring cyclogenesis. The post-monsoon season over the NIO (late September to early December) is known to produce intense cyclonic storms forming from regions of low pressure or troughs embedded within easterly waves having a period of 3 to 4 days (India Meteorological Department, 2016) with a major portion of storms forming over southeast BoB. In addition to these variables, many studies have shown that surface latent heat flux which is associated with sea surface temperature (SST) and surface wind speed is related to cyclogenesis through the air-sea interaction processes (Zhou *et al.*, 2015) and favourable environments with higher moisture consumption through deep convection, enhanced surface fluxes of moisture and kinetic energy, enable storm intensification even in the presence of higher vertical wind shears (Baisya *et al.*, 2020). Warm SST leads to higher surface latent heat flux in turn increasing the surface wind speed (Liu and Curry, 2006), which may act as a positive feedback (Li *et al.*, 2011) aiding in cyclogenesis and storm development under favourable environmental conditions. As this process continues within the storms, the upper ocean provides enough heat energy to the overlying atmospheric boundary layer and for the deepening process (Emanuel, 1999).

A study by Murakami *et al.* (2017) showed a recent increase in frequency of extremely intense cyclonic storms over AS owing to the equatorial NIO warming especially in the post-monsoon period. Very Severe Cyclonic Storm (VSCS) Ockhi is the first storm in almost a century to traverse a rare path forming over southeast BoB and

moving into southwest AS severely affecting the south Indian coasts and Srilanka as it underwent rapid intensification (IMD, 2017). Another low pressure area crossed in to BoB basin as Ockhi attained maximum intensity and it propagated north-north westward towards east coast as a deep depression without developing further. In the first part of the study, different cyclogenesis indices are compared for these 2 storms to understand whether the major controlling and driving factors that affect the cyclogenesis and rapid intensity changes are captured.

In the next part, for storm track prediction from multi-model ensemble prediction system (MMEPS), the model output fields are post-processed in order to identify the accurate storm locations. In this study, the performance of an objective tracking algorithm (Ganesh *et al.*, 2019) based on the Geophysical Fluid Dynamics Laboratory's vortex tracker is analysed for selected storms using reanalysis datasets as inputs. The algorithm considers mean temperature of the warm-core layer, wind speed and vorticity at 850 hPa, minimum sea level pressure, geo-potential height of 200-1000 hPa layer etc. Finally, real-time probabilistic forecasts of cyclogenesis, evolution and track from the prediction system is analysed for two recent tropical cyclones, Amphan and Nisarga using the outputs from MMEPS.

2. Data and methodology

2.1. *Data sets and model*

The NIO basin comprising of AS and BoB is considered as the study area 2 - 25° N and 50 - 100° E. The details of selected storms (Table 1) are obtained from India Meteorological Department (IMD, 2017, 2020) reports and best-track datasets. 6-hourly and daily data of dynamic and thermodynamic variables including *u*, *v*, *w* components of wind, air temperature, relative humidity, SST, mean sea level pressure (MSLP), geo-potential height etc. are obtained ERA-Interim (Berrisford *et al.*, 2011) data at 1° spatial resolution.

The ensemble mean prediction from a multi-model ensemble framework using the nearest Initial Conditions (ICs) to the date of genesis of the storms are shown in the study. Multi-Model Ensembles (MME) include the coupled general circulation model Climate Forecast System version 2 (CFSv2; Saha *et al.*, 2014) and its atmospheric component Global Forecast System (GFS) forced with bias-corrected sea-surface temperature (SST) from CFSv2 (Sahai *et al.*, 2013; Abhilash *et al.*, 2013, 2014a, 2014b, 2014c), both at T126 and T382 horizontal resolutions and is implemented operationally as the CFS-based Grand Ensemble Prediction System (CGEPS) for probabilistic prediction in the extended range by IMD (Pattanaik *et al.*, 2019; Kaur *et al.*, 2020). Atmospheric ICs are provided by National Center for Medium Range Forecast while Indian National Centre for Ocean Information Services (INCOIS) provide the oceanic ICs. Each IC is perturbed to generate 3 additional ICs (Abhilash *et al.*, 2014c). Thus 16 ensemble members are run once every week (Wednesdays) for the next 32 days.

2.2. *Genesis Potential Index*

GPI is a climatological index using potential intensity, relative humidity (H) at 600 hPa, absolute vorticity (η) at 850 hPa and vertical wind shear (V) between 850 and 200 hPa scaled and defined as (Emanuel, 1986; Free *et al.*, 2004):

$$\mathrm{GPI} = \left|10^5\eta\right|^{\frac{3}{2}}\left(\frac{H}{50}\right)^3\left(\frac{\mathrm{Vpot}}{70}\right)^3\left(1+.1V_{\mathrm{shear}}\right)^{-2} \qquad (1)$$

Vpot is the potential intensity in m/s defined as:

$$\mathrm{Vpot}^2 = \frac{C_K}{C_D}\frac{T_S}{T_0}\left(\mathrm{Cape}^a - \mathrm{Cape}^b\right) \qquad (2)$$

where, T_s is the SST, T_0 is the mean temperature at the level of neutral buoyancy, C_K is the exchange coefficient for enthalpy, C_D is a drag coefficient, Cape^a is the convective available potential energy of air lifted from saturation at sea level in reference to the environmental sounding and Cape^b is that of boundary layer air.

2.3. *Genesis potential parameter*

Genesis Potential Parameter (GPP) proposed by Kotal *et al.* (2009), further evaluated (Kotal *et al*., 2013; Nath *et al*., 2013) is implemented operationally by IMD for tropical cyclone monitoring. GPP consist of low-level relative vorticity (ξ at 850 hPa), shear parameter (S) vertical wind shear between 200 and 850 hPa, humidity parameter (M) obtained from scaled middle tropospheric relative humidity (RH) (700-500 hPa) and middle tropospheric instability (I) between 850 and 500 hPa constitutes the KGPP defined as:

$$\mathrm{KGPP} = \frac{\xi 850 \times M \times \mathrm{I}}{\mathrm{S}};\ \text{if } \xi 850 > 0, M > 0\ \&\ I > 0$$

$$= 0;\ \text{if } \xi 850 \le 0, M \le 0\ \&\ I \le 0 \qquad (3)$$

where, $M = \frac{(\mathrm{RH} - 40)}{30}$ and $\mathrm{I} = (T_{850} - T_{500})$

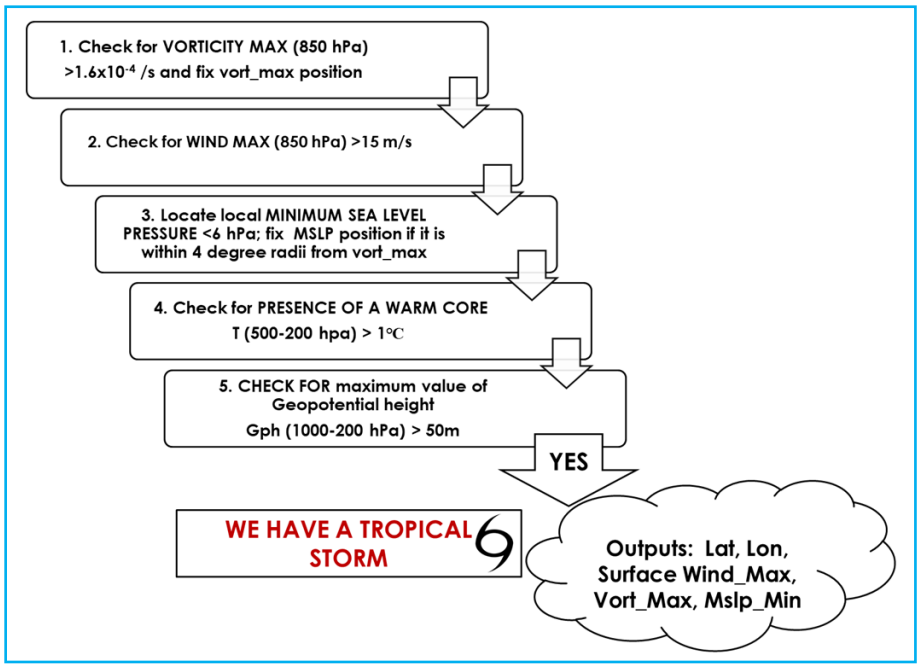

Fig. 2. Schematic diagram for objective tracking algorithm

2.4. *Cyclogenesis and storm evolution parameter*

This parameter is an improved version of GPP (therefore, IGPP) (Ganesh *et al.*, 2020) retaining the vorticity and middle tropospheric humidity terms of KGPP while the thermodynamic term is modified as the scaled and averaged equivalent potential temperature (θe) between 1000 and 500 hPa so as to include the effect of sea surface temperatures, surface heat fluxes and also to include the effect middle tropospheric warming due to latent heat release associated with conditional instabilities or positive feedbacks associated with cyclogenesis. The vertical shear between 850 and 200 hPa is scaled and averaged over an annular region between 100 and 200 km radii for each grid point to highlight the effect of background shear and scaled according to GPI.

where,

$$\text{Thermodynamic term, } I = \frac{(e_{1000} + e_{500})}{2} \quad (4)$$

$$\text{Scaled as; } T = \frac{I - 273.15}{6} \quad (5)$$

Mean middle tropospheric relative humidity,

$$H = \frac{(\text{MRH} - 40)}{30} \quad (6)$$

$$\text{Relative vorticity at 850 hPa, } V = \xi_{850} \times 10^5 \quad (7)$$

Scaled magnitude of vertical wind shear (200-850 hPa) (V_{shear}) averaged over an annular region (Chen and Fang, 2012) between 100 and 200 km from each grid point;

$$S = (1+1V_{shear})^{-2} \quad (8)$$

Thus, IGPP is defined as:

$$\text{IGPP} = V \times H \times T \times S, \text{ where, } V > 0, H > 0, T>0, S>0$$

$$= 0, \text{ otherwise.} \quad (9)$$

2.5. *Objective tracking Algorithm*

The CGEPS MME is found to be skilful and reliable in the prediction of monsoon intra-seasonal oscillations, Madden-Julian Oscillations (MJO) and extreme weather events (Sahai *et al.*, 2013, 2016; Joseph *et al.*, 2015). Here, a modified version of vortex tracking scheme by GFDL is implemented to generate the track positions from ensemble outputs (Ganesh *et al.*, 2018, 2019). Major parameters used for storm identification are wind-speed and vorticity at 850 hPa, minimum sea level pressure, mean temperature of the warm-core layer between 200 and 500 hPa layers and geo-potential

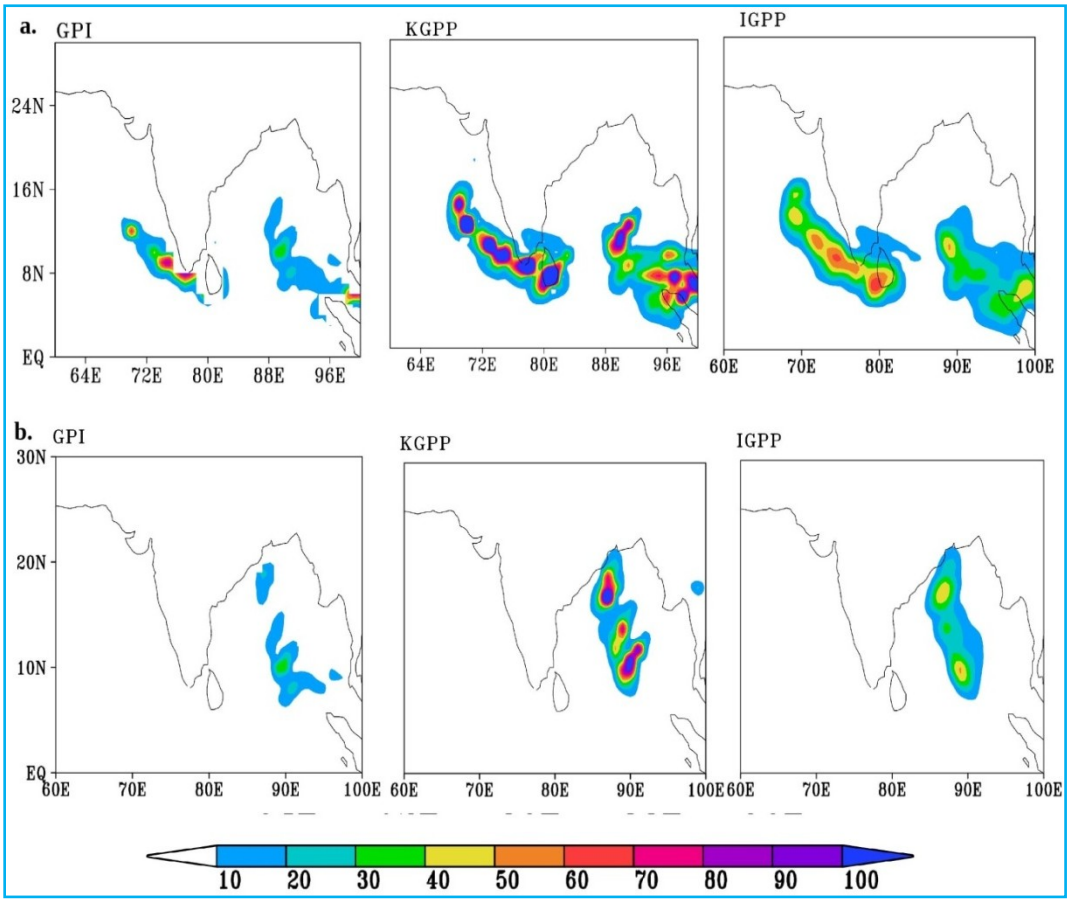

Figs. 3(a&b). Maximum values of Genesis indices GPI (column 1), KGPP (column 2), IGPP (last column) for (a) VSCS Ockhi from 29 November to 5th December and (b) DD from 5th to 9th December

thickness of 200 to 1000 hPa layer. The basic algorithm is shown in Fig. 2. Space-time threshold criteria are set for each parameter chosen as predictor and the algorithm is applied on all 16 members of MME. A storm is identified only if a minimum of 4 members of the ensemble group can locate the cyclone centre location by satisfying all the conditions of the algorithm. From this, the MME-mean as well as ensemble track positions are obtained as outputs. The model derived tracks are verified using IMD best track datasets.

3. Results and discussion

3.1. *Cyclogenesis potential parameters and the storm evolution - A case study*

The maximum values of each indices selected, GPI, KGPP and IGPP are plotted for the entire evolution of the storms, from 29th November to 5th December for Ockhi and from 5th to 10th December for the DD [Figs. 3(a&b)]. GPI developed by Emanuel and Nolan, 2004 is a climatological index based on Gray's parameters. It is found that GPI values are accurately showing the cyclogenesis, but cannot be used for monitoring the evolution of individual storms as the value reduces after the initial stage of the storm. This is the case for both Ockhi and DD as GPI could capture the genesis stage.

A drawback of GPI when used for cyclogenesis monitoring on daily timescales over a narrow basin such as NIO is that, due to the potential intensity term which includes the ocean parameter to show the effect of sea surface temperature, GPI is unable to capture the cyclogenesis or rapid development occurring in close proximity to the coasts. To understand the reason behind the low values of GPI during the intensification and evolution of the storms, its constituent parameters are plotted for the entire evolution of Ockhi. Absolute vorticity distribution (Fig. 4 - Left) is similar to initial GPI distribution, but reaches maximum values on December 4 contrary to GPI. By December 5, the vorticity field also shows the dissipation stage of Ockhi under the influence of the large-scale flow. The distribution of mid-tropospheric humidity (Fig. 4 - Right) during the genesis of

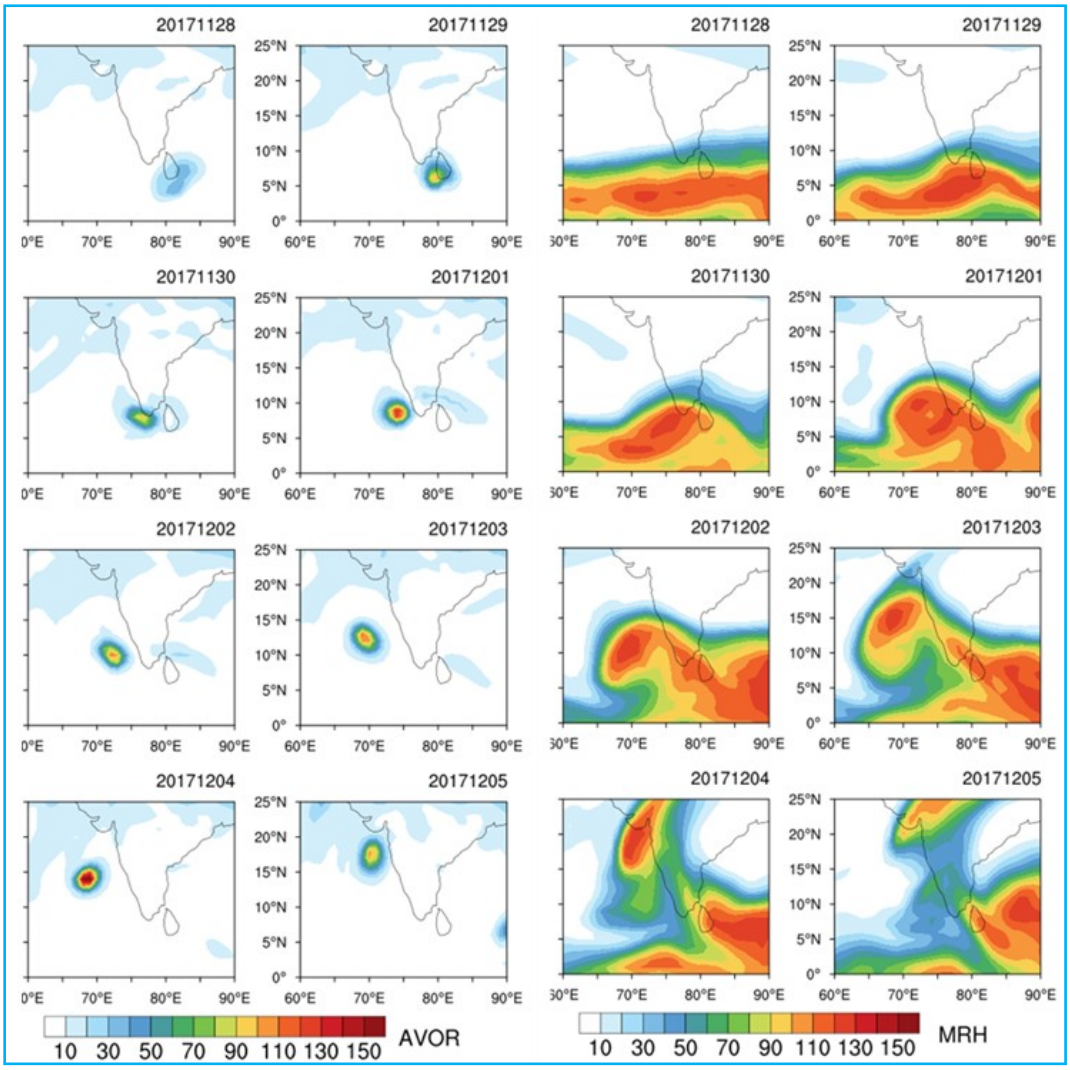

Fig. 4. Scaled values of observed Absolute vorticity (left) and Mid-tropospheric Relative humidity (right) from GPI for VSCS Ockhi from 28th November to 5th December, 2017

the storm near the equatorial region is similar to that of an easterly wave propagation and Marsupial theory of storm formation and Genesis (Rajasree *et al.*, 2013; Dunkerton *et al.*, 2008) where, the easterly wave troughs provide favourable "seedling" circulations for a large proportion of tropical cyclones similar to observed moisture distribution during the evolution of Ockhi up to December 3, after which the storm gets detached from the large-scale humidity environment in the equatorial region.

The maximum value of potential intensity distribution (Fig. 5 - Left) during the genesis stage is within the range of 21 and there is no clear impact of potential intensity term at the time rapid intensification from 29 November to 1 December. However, after December 2, with the progression of storm towards northwest, a pattern of very low Vmax is visible along the trail of storm, which apparently reflect the reduction in SST over the region after the storm passage due to upwelling and upper ocean response (Ganesh *et al.*, 2019). This affected the GPI performance after December 2 leading to lower values, as potential intensity clearly manifests the effect of sea surface temperatures and sea-surface cooling by upwelling (Chen and Liu, 2014; Kikuchi and Wang, 2010). Montgomery *et al.* (2008) suggested that decreasing translational speed along with high storm intensity can lead to larger upper ocean response.

According to IMD, Ockhi had a 12-hour average translational speed of 15 km/h which satisfy the slow-moving criteria until its mature stage. Minimum potential intensity value is observed on 4 December when the storm

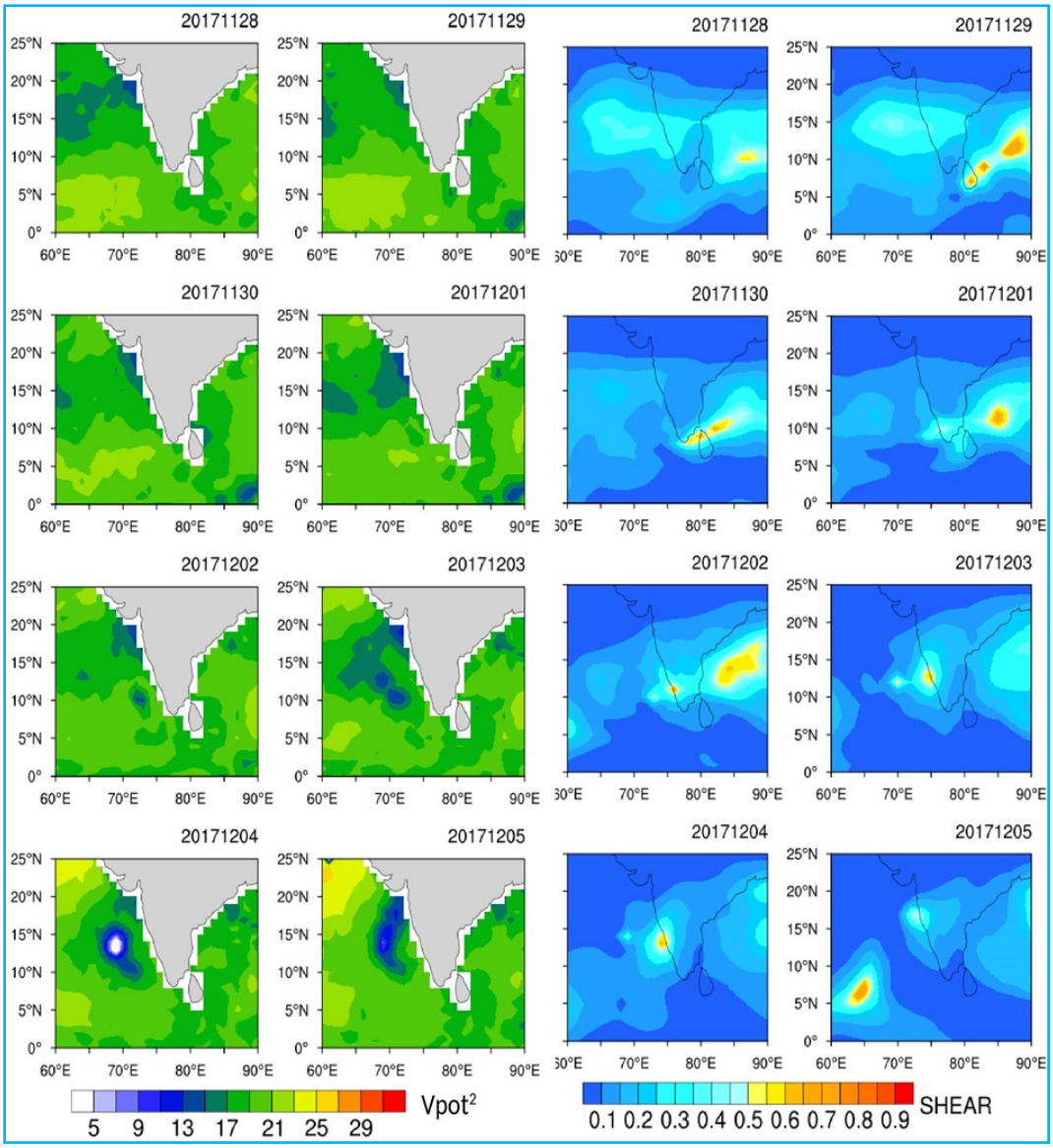

Fig. 5. Potential Intensity term (left) and vertical wind shear (right) from GPI during the life-cycle of VSCS Ockhi

had its peak intensity and gradually changed its course to northeast, which is again reflected in the GPI spread on that day. So, it is concluded that, while maximum potential intensity is a crucial parameter which represents the pre-existing thermodynamic state of ocean and boundary layer in the inter-annual, annual, seasonal and climatological time-scales to monitor cyclogenesis over major ocean basins, it may not be helpful in real-time prediction of NIO storms that may undergo rapid intensity changes close to the coasts or to capture the evolution of intense slow-moving storms. The vertical wind shear term (Fig. 5 - Right) had low values in the vicinity of the storm during its genesis and intensification. Whereas, as it progressed north-westward, near 15° N, a large area of positive shear is visible which gradually evolved with time leading to the rapid dissipation of the storm. The system, under the influence of this shear induced by upper-level westerlies, thus underwent recurvature and steered northeast towards the Indian Coast.

Similar patterns were observed for the evolution of DD which could not develop due to the higher vertical wind shears. KGPP uses only atmospheric parameters and thus could capture the entire evolution of the storms. IMD keeps the scale of KGPP up to 30, as the threshold value and that, higher KGPP values show the potential zone of cyclogenesis. However, it is evident from the figures that, when the scale is increased, the

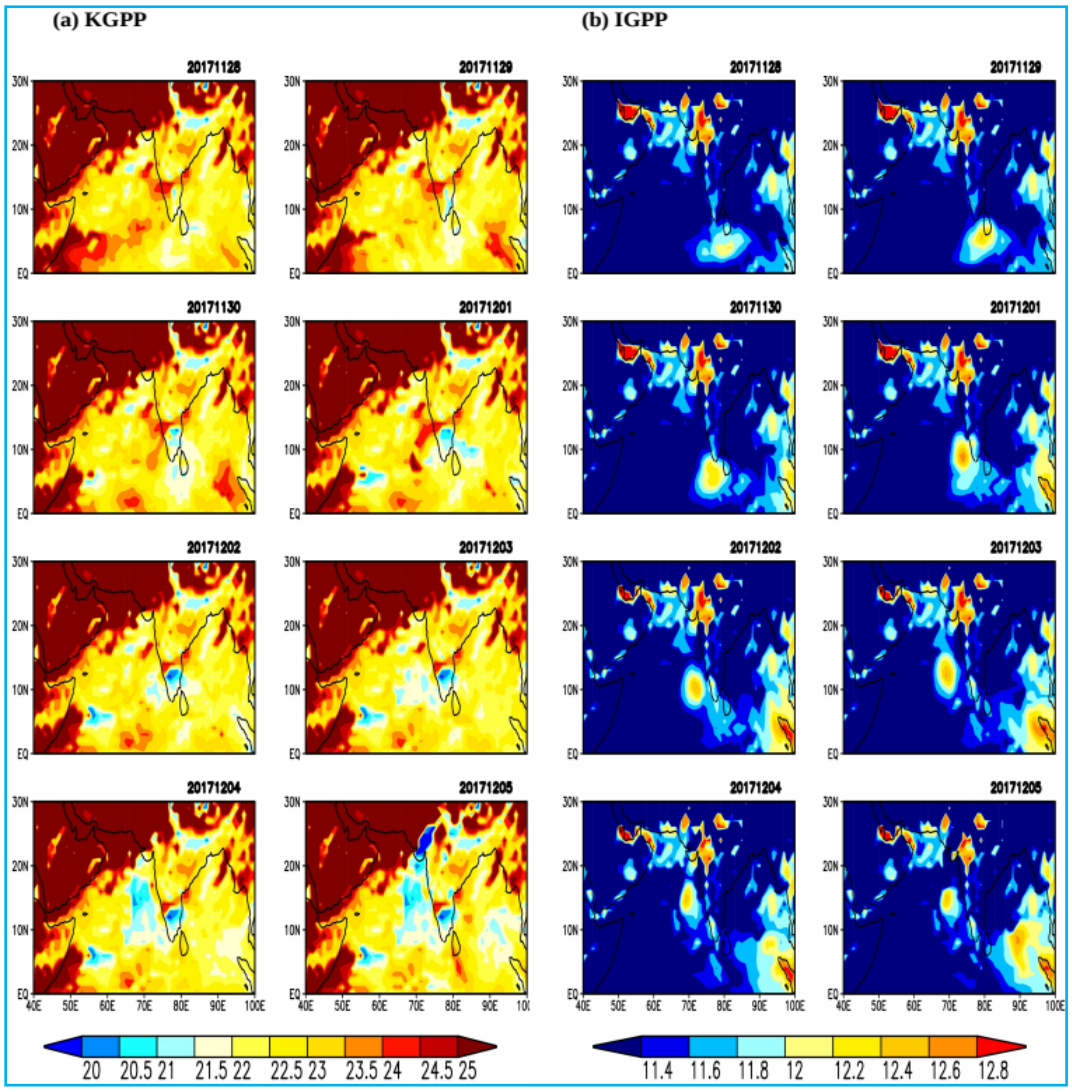

Figs. 6(a&b). Evolution of thermodynamic term used by (a) KGPP and (b) IGPP for VSCS Ockhi from 28th November to 5th December, 2017

maximum values of the GPP are higher than other indices with increased number of false alarms over regions where the low pressure areas initially developed. The IGPP however captures the genesis, intensification and dissipation of the storms without false alarms or overestimations. It is interesting to note that, for DD, maximum values of index never exceeded 60. The analysis of constituent parameters of GPI and GPPs will further help to understand the parameters creating false alarms in KGPP and the reason for improvements in IGPP. Comparison of the thermodynamic terms from KGPP and IGPP [Figs. 6&7(a&b)] show that thermal instability term decreases with the increase in storm intensity. It is also clear that other than vorticity parameter, all other variables are contributing to the overestimation of KGPP values observed over BoB.

3.1.1. *Storm prediction from MME using the nearest ICs from the cyclogenesis date, KGPP vs IGPP*

To check how the GPPs for NIO have predicted the evolution of Ockhi and DD from the operational MMEPS, nearest model runs from the date of storm genesis are used. For Ockhi, 29 November IC and for DD, 6 December IC predictions are plotted [Fig. 8(a)] for the entire evolution of the storms and observed best-tracks are overlaid for comparison. One noticeable difference between analysis and prediction is that the GPP values are much lower in the MME mean outputs compared to analysis. This may be due to the result of ensemble spread or due to underestimation of predicted values with increasing lead time (Ganesh *et al.*, 2019). Hence, the

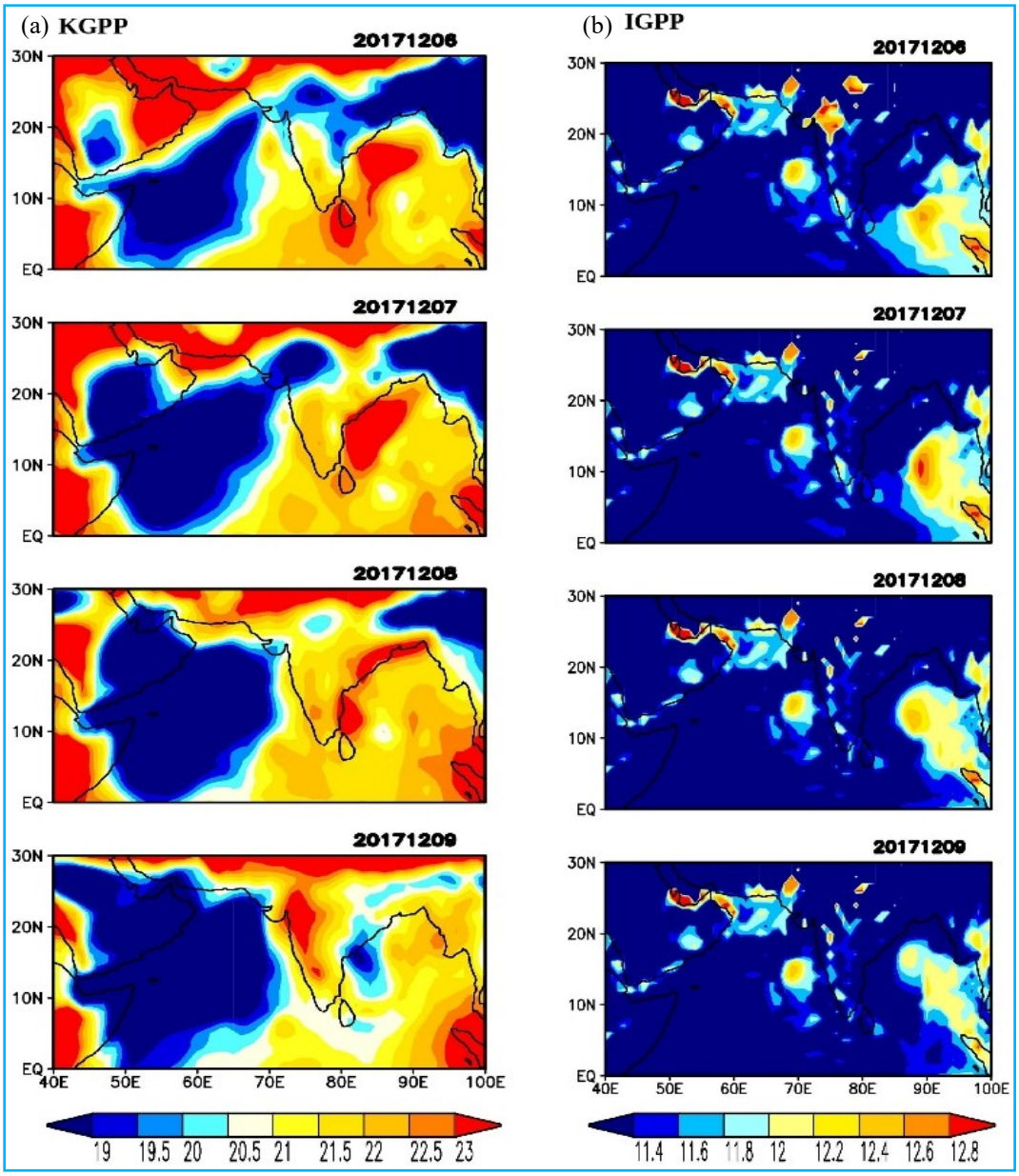

Figs. 7(a&b). Same as Fig. 6, but for DD from 6-9 December, 2017

scale is reduced by half in figures. Even then, similar to the analysis, the values are higher for KGPP prediction with persisting false alarms over BoB making it difficult to understand whether the storm system over AS or that over BoB will develop which may lead to misinterpretation in prediction. These false alarms and overestimations are completely absent for IGPP predictions and the values are high and closely following the path that Ockhi traversed. This clearly shows that changing the thermodynamic and shear parameters could indeed improve the GPP, thereby improving both the analysis as well as the MME predictions by reducing the false alarms and capturing the storm evolution with reasonably good skill. Similar predictions are obtained for the DD that developed over BoB following Ockhi. It is remarkable that IGPP is better than KGPP in distinguishing between strong and weak storms by being able to eliminate the overestimated values present for KGPP for the case of DD. Thus, it can be concluded that the implementation of IGPP for probabilistic prediction of cyclogenesis and evolution over NIO will definitely provide a better guidance from MME with reduced false alarms and better representation of the evolution of storms.

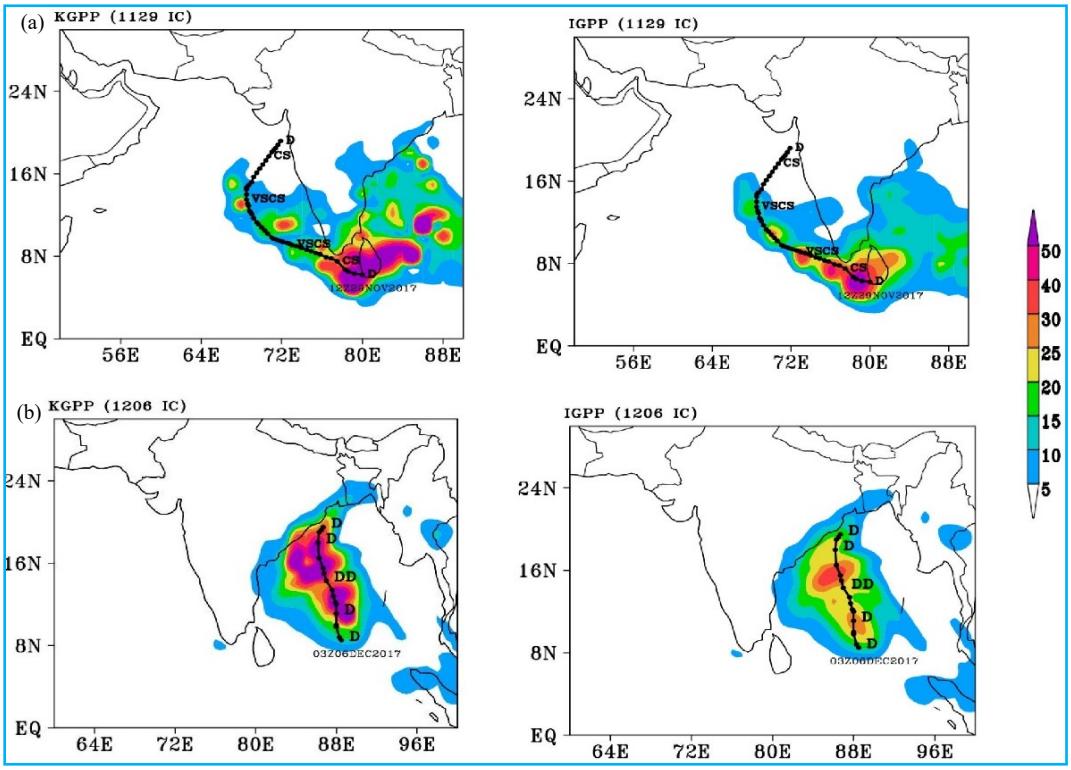

Figs. 8(a&b). Predictions from MME using nearest IC from the date of genesis KGPP (left), IGPP (right) for (a) Ockhi and (b) DD

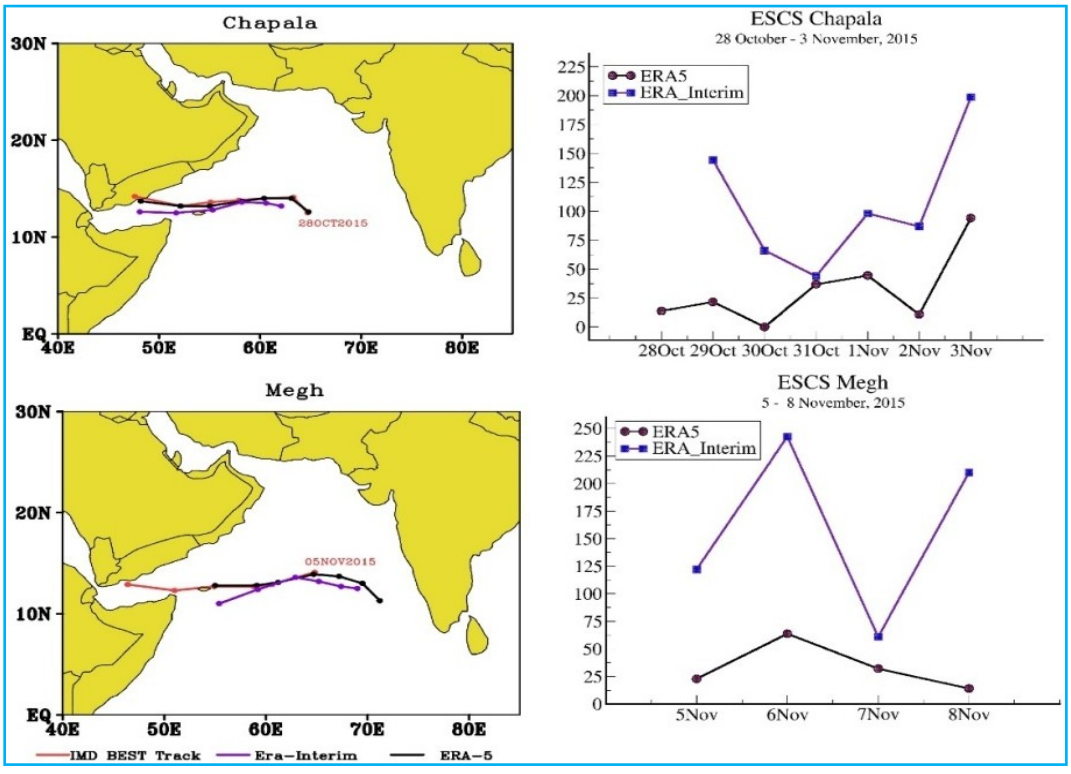

Fig. 9. Tracks of ERA_interim and ERA5 from objective tracking algorithm compared with IMD best tracks (left column) and corresponding direct position errors (kms) (right column) for Chapala (row 1) and Megh (row 2)

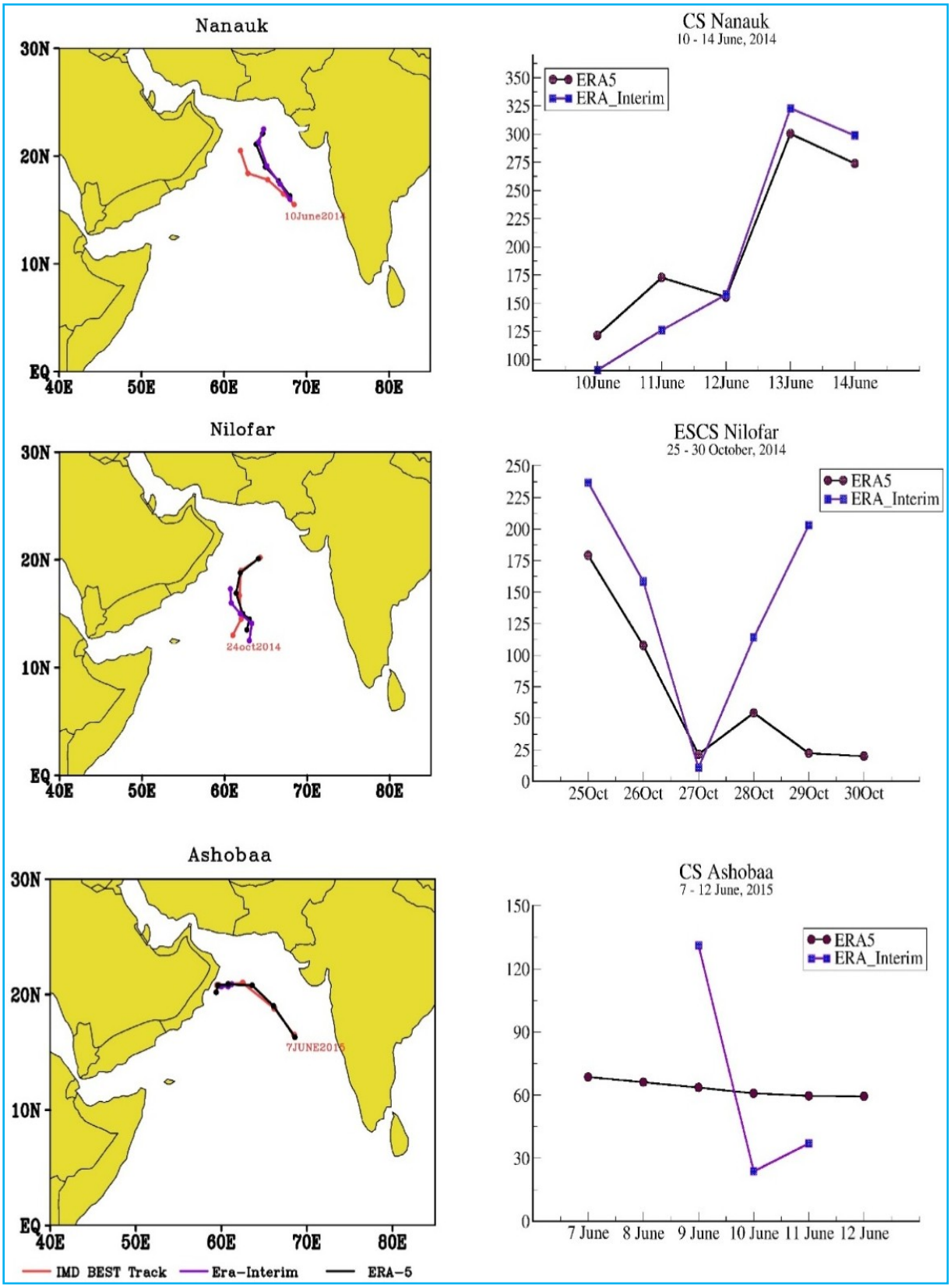

Fig. 10. Same as Fig. 9, but for (top to bottom) Nanauk, Nilofar and Ashobaa

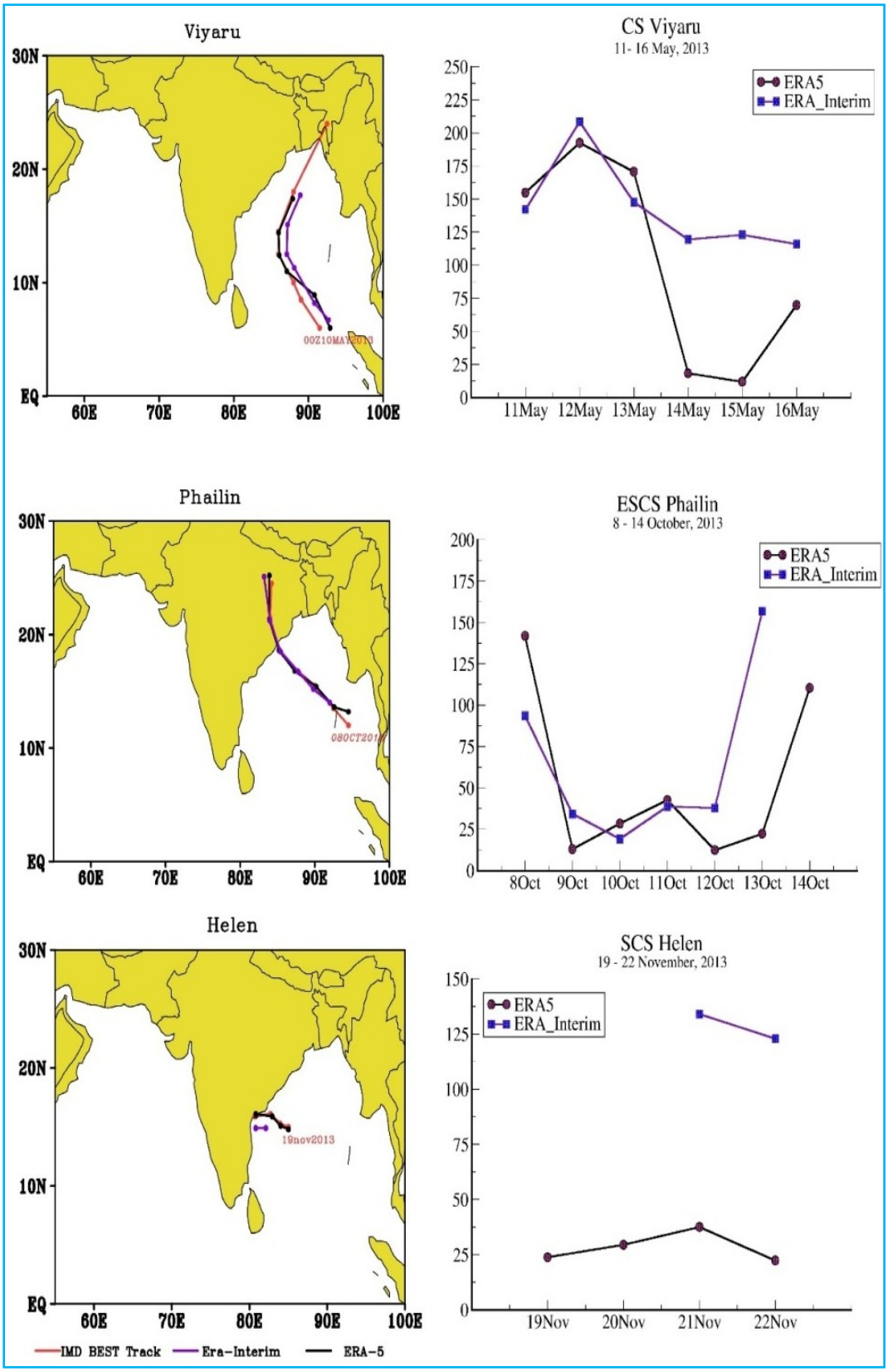

Fig. 11. Same as Fig. 9, but for (top to bottom) Viyaru, Phailin and Helen

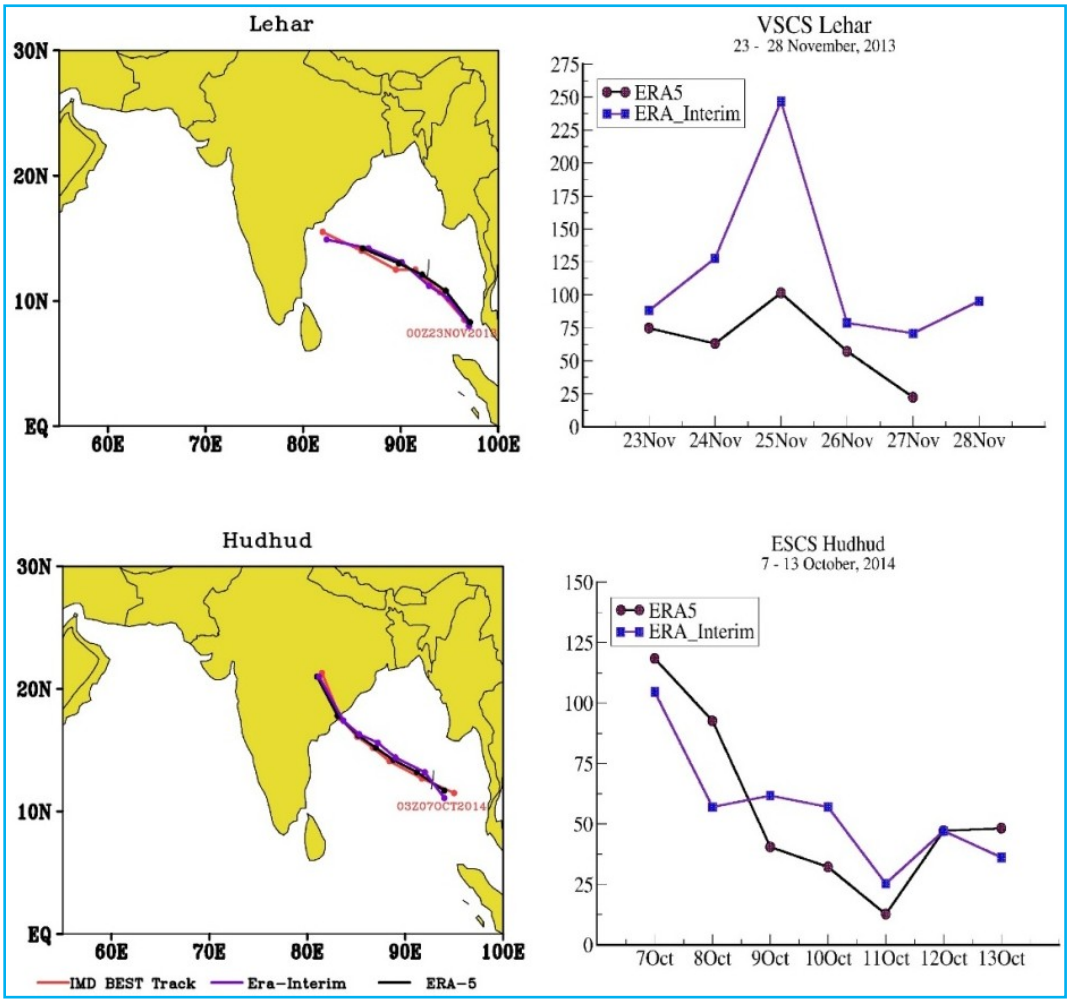

Fig. 12. Same as Fig. 9, but for Lehar (row 1) and Hudhud (row 2)

3.2. *Performance of the objective tracking algorithm : Observations vs Re-analysis products*

To check the performance of objective tracking algorithm developed for detecting storm tracks from MME hindcasts, 10 storms (Table 1, Rows 5-14) of which five that formed over AS and five that formed over BoB from the years 2013 to 2015 are chosen. The two widely used ECMWF re-analyses; Era-Interim and ERA-5 daily averaged datasets, considered as two of the best available reanalysis datasets with reasonable accuracy are used as inputs in the algorithm. The tracks produced by the algorithm for selected cases are further verified using IMD best-track data and corresponding positional track errors are calculated for each case.

For ESCS Chapala and Megh (Fig. 9), ERA5 storm tracks follow the IMD best tracks without much position errors, while the ERA-Interim tracks are diverging and inconsistent. The genesis location of Chapala could not be captured from ERA-Interim data, but are better captured by ERA-5. The location of cyclogenesis of Megh and its further movement is better captured by the algorithm from ERA5 datasets even before IMD started tracking the locations from the Depression stage. Fig. 10 shows the track predictions of pre-monsoon cyclones Nanauk, Ashobaa and post-monsoon ESCS Nilofar. For the case of Nanauk, tracks detected from both datasets are matching each other whereas the best track has diverged away three days after the cyclogenesis. This is also shown by a sharp increase in the DPE values to more than 300 km on 13 June. For Nilofar, some changes in the genesis location are observed in both tracks captured by the algorithm. However, ERA-5 tracks are accurately following the best track afterwards with track errors reducing below 50 km from third day. Track locations for Ashobaa from Era-Interim dataset were detected only on three days: June 9,

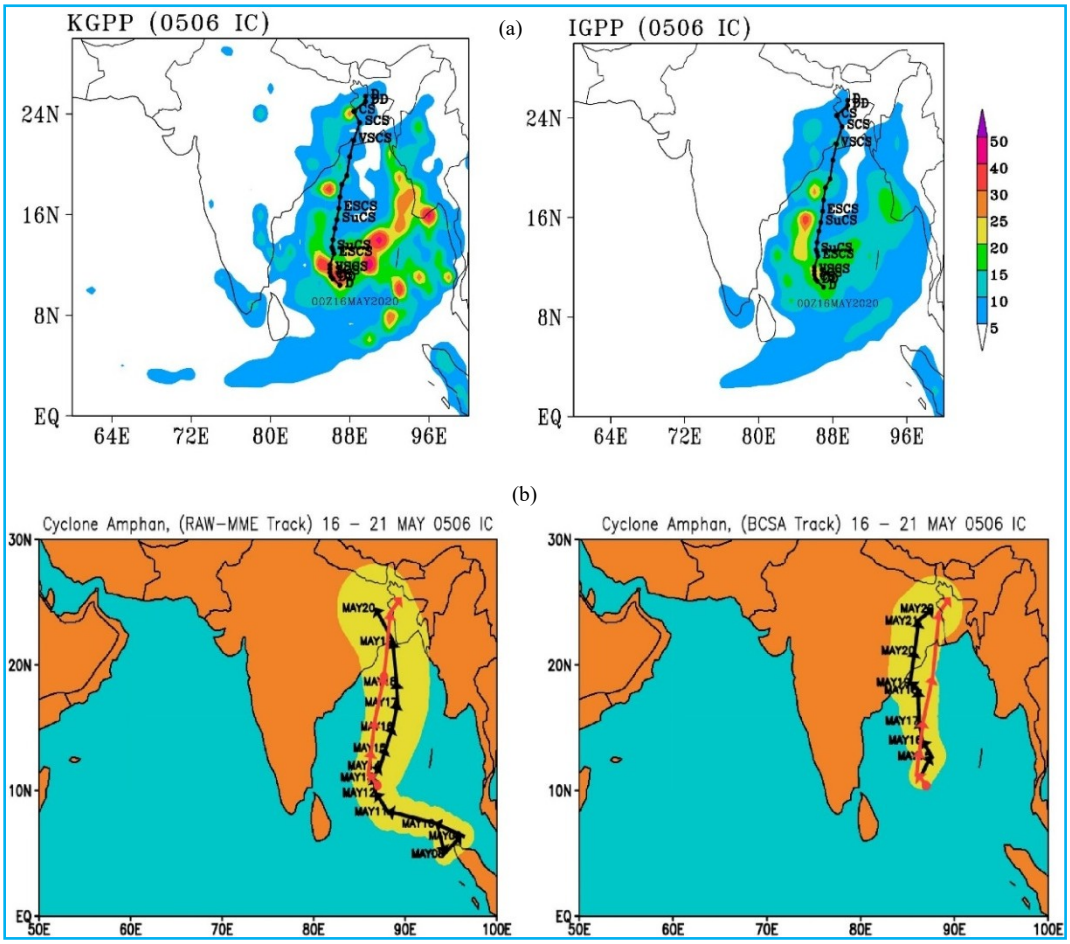

Figs. 13(a&b). (a) Predicted KGPP and IGPP evolution from 6 MAY IC for Amphan with observed track overlaid from 16 to 21 May, 2020; (b) Predicted (black) *vs* IMD best track (red) for cyclone Amphan from MME-RAW(left) and MME-BCSA (right)

10 and 11 after the storm attained maximum intensity and before it started dissipating. Still, the ERA5 tracks have very less errors of approximately 60 km. The slight differences in the observed and ERA5 tracks are almost illegible in the track plots and DPE also show a slightly decreasing trend with time and the track is closely following the observed track.

The storms that formed over BoB basin are shown in Figs. 11&12. Track plots of Viyaru, Phailin, Hudhud, Helen and Lehar show that, the tracks detected by the algorithm from both re-analyses are at par with the observed tracks. In the case of Viyaru, the locations are shifted to the east of the observed point initially, but ERA5 tracks follows the observed tracks from the third day. The shape of the ERA-Interim track is similar to the other tracks, but the initial eastward shift of about 1 degree is persisting throughout. For Helen also, the algorithm could not detect track positions from ERA-Interim data whereas a perfect track with DPE of almost 40 km and lesser is obtained from ERA-5 datasets. For the cases of Phailin and Hudhud, there are some position errors in the initial and final days and ERA-Interim track is more similar to ERA5 track compared to other cases. In some storms such as Viyaru, Megh, Lehar and Nilofar, it is observed that the tracks produced by the algorithm are shorter than the IMD best storm tracks. This is because even though the lower level vorticity and minimum pressure criteria may be satisfied, all of the thresholds and criteria may not be followed in the datasets throughout the entire lifetime of the storms (Camargo and Zebiak, 2002). Such datasets will not be helpful in studying tropical storm track and intensities. Hence, analysis prove ERA-5 datasets to be better than ERA-Interim, both in capturing the accurate storm locations and also the proper life time of the storms. It is also evident that objective tracking algorithm is well capable of producing skillful tracks from the input datasets.

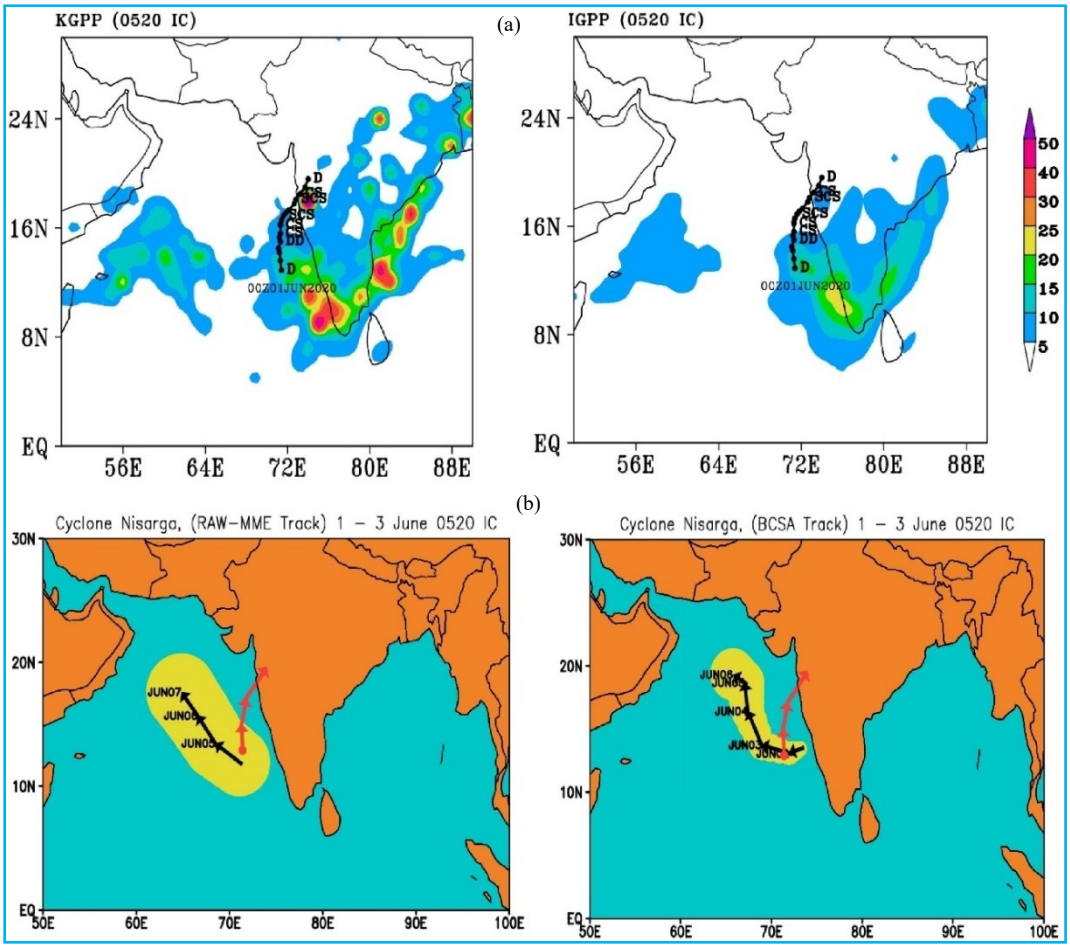

Figs. 14(a&b). Same as Fig. 13, but for SCS Nisarga from 1 to 3 June, 2020 using 20 May IC

3.3. *Real-time probabilistic prediction of recent tropical cyclones from MMEPS*

Based on the prediction system explained in the previous sections, the performance of CGEPS-MME in the prediction of two recent pre-monsoon storms, Super Cyclone Amphan and Severe Cyclone Nisarga is discussed.

Super Cyclone, Amphan developed from a depression that formed on May 16, 2020 over south east BoB. The low pressure system that evolved in to Amphan formed on 13 May and persisted over warm central BoB slowly gaining energy. Fig. 13(a) shows the comparison of cyclogenesis and evolution predictions using KGPP and IGPP from 6 May IC MME mean outputs along with IMD best-track overlaid. The spread in the ensembles are well evident as the forecast is having more than 10 days lead. This spread show the probability of storm evolution towards both northwards and north-northeast while the actual storm path is northward. KGPP is showing higher values towards northeast and Myanmar coasts which is in turn the false alarm that is successfully eliminated by IGPP. For IGPP, the values does not exceed 20 over the region of false alarms, moreover, it shows higher values of 30 and 40 over the location where the storm rapidly intensified into super cyclone. Even though MME mean values are not very high, the fact that IGPP MMEPS could capture not only the cyclogenesis but also the probable evolution from MMEPS almost 10 to 16 days in advance is itself a remarkable achievement. Track predictions [Fig. 13(b)] using the MME outputs from 6th May IC also closely captures the probable movement of the storm accurately. To reduce the space-time errors in storm track prediction, a post-processing technique involving climatological bias-correction and signal amplification (BCSA) (Ganesh *et al.*, 2018; Chattopadhyay *et al.*, 2020) is applied on the MME outputs in order to reducing large ensemble spread or uncertainties in the outputs. The predicted tracks from objective tracking algorithm using MME-raw and MME-BCSA outputs and observed tracks for Amphan show that MME-BCSA mean could capture

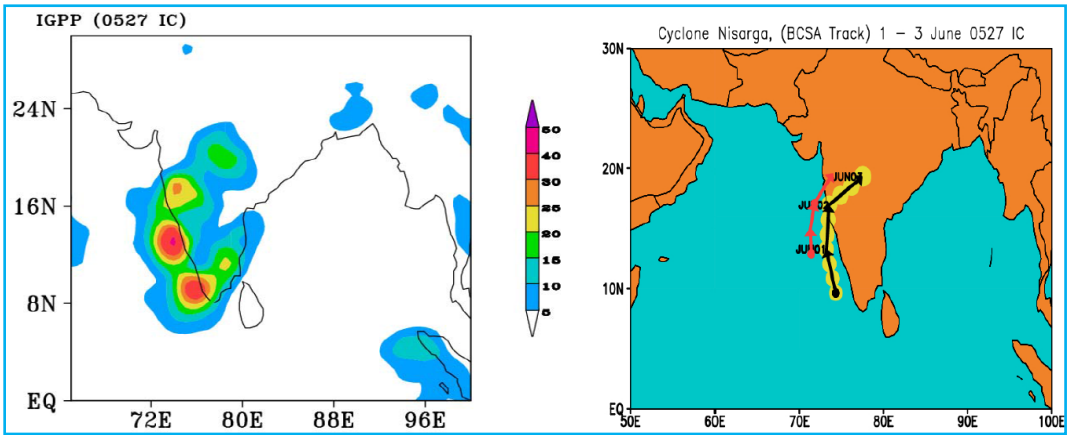

Fig. 15. Predicted IGPP evolution and track for Nisarga using MME-BCSA outputs at 27 May IC from 31 May to 3 June, 2020

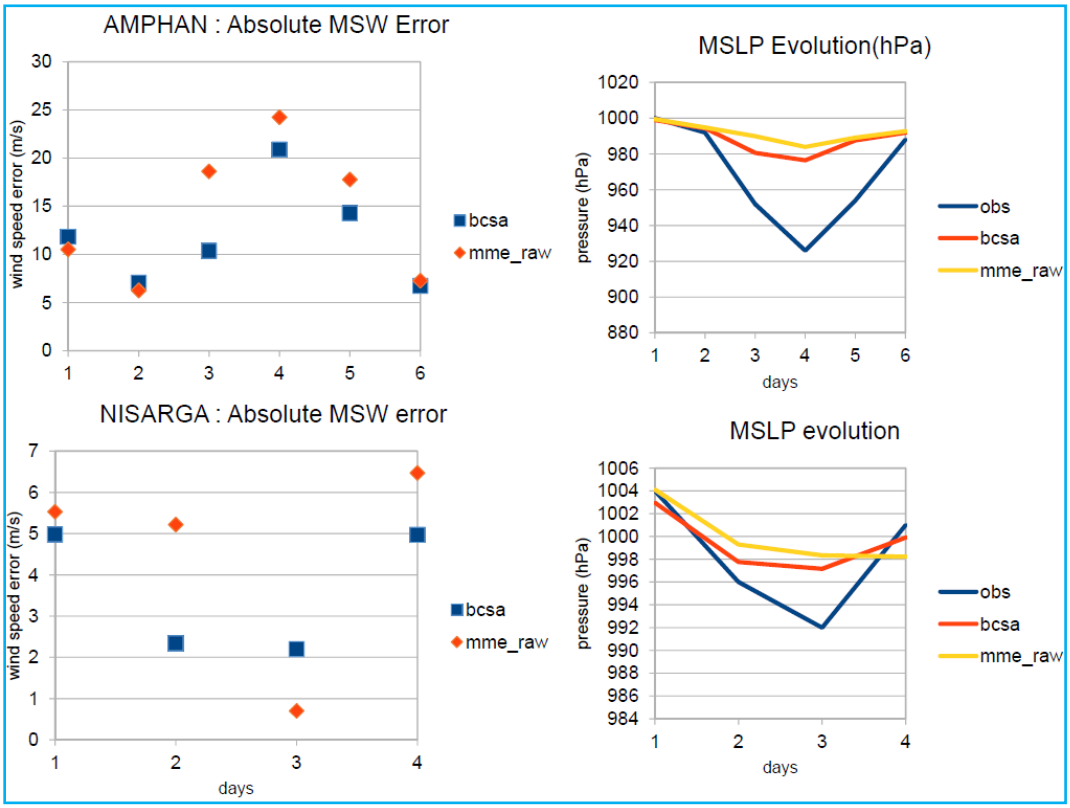

Fig. 16. Absolute MSW errors (m/s) and MSLP evolution for Amphan, from 16 to 21 May with predictions from 6 May IC (row 1) and Nisarga, from 31 May to 3 June using predictions from 20 May IC (row 2)

the genesis location as well as the storm evolution and cone of uncertainty better than the MME-raw further improving the track forecast at 6 May IC.

Severe Cyclonic Storm Nisarga formed from the summer monsoon onset vortex over southeast AS and adjoining South Indian Peninsula on 31 May, 2020. The system slowly propagated north-northwest ward and recurved towards the west coast of Peninsular India and crossed Maharashtra coast on June 2 at its peak intensity. The MME-mean predictions of cyclogenesis and evolution as well as storm tracks from MME-raw and MME-BCSA mean shown here are based on 20 May IC, almost 10 days ahead of the genesis of the storm [Figs. 14(a&)]. For Nisarga, the genesis location of the low pressure over southeast AS is captured by both KGPP

and IGPP, but, similar to previous cases, the values are overestimated by KGPP along the east coast of India and over west AS as well as high values over the region of low-pressure, *i.e*., the onset vortex. The False alarms are perfectly eliminated in IGPP evolution with values below 20 both over land and ocean. Even though both GPP had weak signals of cyclogenesis over southeast AS, IGPP showed values up to 25 for the onset-vortex, lower and more accurate when compared to the unscaled KGPP. The tracks predicted from MME-raw mean outputs are a bit diverging and moving northwest towards central AS while this positional error could be reduced a little using MME-BCSA mean outputs for which, a more northward track is predicted by the algorithm. These results show that, the predictability from 10-day lead or more is lower for Nisarga than for Amphan which may be due to the absence of local-scale air-sea interaction processes that led to the genesis of low pressure over southeast AS in the IC as well as the strong influence of effects of large scale climatological monsoon flow in the climate models used in MMEPS (Ganesh *et al.*, 2019). Since Nisarga is a weaker and short-lived (3 days lifetime) storm, the predicted IGPP evolution and MME-BCSA tracks are plotted using nearest IC, MME outputs (27 May IC) in Fig. 15. Predictions from 27 May IC has accurately captured the both the evolution and track with little spatial errors. Hence, it is evident having accurate and nearest possible ICs from cyclogenesis date is crucial for the accurate forecast for tropical storm evolution. The maximum surface wind (MSW) errors and MSLP evolution in the forecasts for Amphan (6 May IC) and Nisarga (20 May IC) are also compared (Fig. 16) for MME-raw and MME-BCSA outputs which reveal that MME-BCSA has reduced errors compared to MME-raw for both cases. Both MSW and MSLP Errors are higher in the case of Amphan on the 3rd and 4th days, when it reached its maximum intensity as Super Cylcone, which could not be captured in the predictions from 6 May IC with a lead time of almost 2 weeks in advance. Analysis of both these cases show the capability of the presently developed storm prediction system for NIO with remarkable improvements in the cyclogenesis, evolution and track predictions. It is also interesting to note that CGEPS-MME is having reasonably good skill in capturing the signals of the development of intense, long-lived storms as compared to weaker, short-lived storms, especially in the extended range perspective, even more than 2 weeks.

4. Conclusions

A detailed review and analysis of the performance of a prediction system developed for the extended range prediction of NIO cyclogenesis and evolution is provided in this article. First, genesis and evolution of two consecutive storms, VSCS Ockhi and the DD that followed are studied using presently available genesis potential indices, GPI, KGPP used by IMD in real-time and in-house developed IGPP to understand the major defining parameters that affect the cyclogenesis and rapid evolution over NIO. Ockhi had an unusual track, as it formed over southwest BoB and moved westward through equatorial Indian Ocean in to the AS. During its life-cycle, the VSCS Ockhi exhibited rare dynamics like rapid intensification in its genesis stage, recurvature and rapid dissipation. GPI could capture the pre-genesis and genesis stages, while both KGPP and IGPP could capture the entire storm evolution. Analyses also reveal the reason that GPI may not be suitable as a real-time predictor of cyclogenesis and evolution due to the SST and potential intensity term. While potential intensity term is vital in producing favourable pre-genesis conditions, it shows an inverse relation to storm intensity due to sea surface cooling owing to the intensity of storm and precipitation. The major drawbacks of KGPP are the overestimated values and presence of false alarms even from the pre-genesis stage for both storms analysed which are rectified by IGPP by using scaled and averaged value of θe which indirectly represent the effect of both sea surface and middle tropospheric warming, as well as the scaled and annular averaged vertical wind shear term. Initial results thus prove that, improving the GPP could indeed lead to better representation of storm genesis and evolution with reduced false alarms in the analysis as well as predictions from MME from nearest IC and thus may be utilized for improving the short, medium and extended range prediction of NIO tropical storms.

Next, an analysis of the modified objective tracking algorithm for storm track prediction from MMEPS is done using different reanalysis datasets. Lower level vorticity, wind speed, thickness of warm core layer, geopotential thickness and MSLP are selected as the predictors in the algorithm by giving appropriate space-time threshold values and criteria for each predictor to capture accurate storm locations at each lead time. Tests involving ERA-Interim and ERA5 daily averaged datasets as inputs to the algorithm for selected storms reveal that the tracks captured by the algorithm are almost as good as the IMD observed tracks. ERA5 datasets produce better tracks with minimal errors compared to ERA-Interim tracks.

Finally, the performance of this prediction system when applied to the real-time probabilistic prediction of two recent tropical cyclones, Amphan and Nisarga is described in detail. The improved skill of the prediction as well as analysis while using IGPP instead of KGPP and the skill of MME-BCSA over MME-raw while used in the prediction system is evident from the analyses, even for predictions having 10 days or more lead time. The

MMEPS is found to be useful in capturing the cyclogenesis and development features of stronger storms, even at longer lead times. The implementation of the IGPP as well as the post-processing technique involving BCSA to improve track prediction from algorithm further refine the outputs by reducing the false alarms, accurately capturing the region of storm evolution with reduced errors in tracks and intensity, thus proving the prediction system to be reliable in the real-time extended range prediction of NIO tropical cyclones. A more detailed study on MMEPS, focusing on the probabilistic and deterministic skills of the MMEPS in capturing the climatological cyclogenesis over BoB and AS based on IGPP by using predictions from weekly ICs during pre-monsoon, monsoon and post-monsoon seasons for recent years will be carried out in the near future.

Acknowledgments

The support of IITM, an autonomous institute under Ministry of Earth Sciences (MoES), as well as support from scientists, researchers, technical support staffs and operational forecasters who are directly or indirectly involved in National Monsoon Mission are acknowledged. The CFS model-based forecast system is implemented as a part of MoU between MoES, Govt. of India and NOAA, US. The contents and views expressed in this research paper are the views of the authors and do not necessarily reflect the views of their organizations.

References

Abhilash, S., Sahai, A. K., Borah, N., Chattopadhyay, R., Joseph, S., Sharmila, S., De, S. and Goswami, B. N., 2014a, "Does bias correction in the forecasted SST improve the extended range pre-diction skill of active-break spells of Indian summer monsoon rainfall?", *Atmospheric Science Letters*, **15**, 2, 114-119. https://doi.org/10.1002/asl2.477.

Abhilash, S., Sahai, A. K., Borah, N., Chattopadhyay, R., Joseph, S., Sharmila, S., De, S., Goswami, B. N. and Kumar, A., 2014b, "Prediction and monitoring of monsoon intraseasonal oscillations over Indian monsoon region in an ensemble prediction system using CFSv2", *Climate Dynamics*, **42**, 9-10, 2801-2815. https://doi.org/10.1007/s00382-013-2045-9.

Abhilash, S., Sahai, A. K., Pattnaik, S. and De, S., 2013, "Predictability during active break phases of Indian summer monsoon in an ensemble prediction system using climate forecast system", *Journal of Atmospheric and Solar-Terrestrial Physics*, **100-101**, 13-23. doi:10.1016/j.jastp.2013.03.017.

Abhilash, S., Sahai, A. K., Pattnaik, S., Goswami, B. N. and Kumar, A., 2014c, "Extended range prediction of active-break spells of Indian summer monsoon rainfall using an ensemble prediction system in NCEP climate forecast system", *International Journal of Climatology*, **34**, 1, 98-113. https://doi.org/10.1002/joc.3668.

Baisya, H., Pattnaik, S. and Chakraborty, T., 2020, "A coupled modeling approach to understand ocean coupling and energetics of tropical cyclones in the Bay of Bengal basin", *Atmospheric Research*. https://doi.org/10.1016/j.atmosres.2020.105092.

Berrisford, P., Dee, D., Poli, P., Brugge, R., Fielding, K., Fuentes, M., Kallberg, P., Kobayashi, S., Uppala, S. and Simmons, A., 2011, "The ERA-Interim archive, version 2.0", ERA report series 1. Reading, Bershire : ECMWF.

Camargo, S. J. and Zebiak, S. E., 2002, "Improving the detection and tracking of tropical cyclones in atmospheric general circulation models", *Weather and forecasting*, **17**, 6, 1152-1162.

Camargo, Suzana J., Kerry A. Emanuel and Adam H. Sobel., 2007, "Use of a genesis potential index to diagnose ENSO effects on tropical cyclone genesis", *Journal of Climate*, **20**, 19, 4819-4834.

Chattopadhyay, R., Joseph, S., Abhilash, S., Mandal, R., Dey, A., Phani, R., Ganesh, S., Kaur, M., Pattanaik, D. R. and Sahai, A. K., 2019, "Understanding the intraseasonal variability over Indian region and development of an operational extended range prediction system", *MAUSAM*, **70**, 1, 31-56.

Chen, S. H. and Liu, Y. C., 2014, "The relation between dry vortex merger and tropical cyclone genesis over the Atlantic Ocean", *Journal Geophys. Res. Atmos.*, **119**, 11641-11661, doi : 10.1002 /2014JD021749.

DeMaria, Mark, John A. Knaff and Bernadette H. Connell, 2001, "A tropical cyclone genesis parameter for the tropical Atlantic", *Weather and Forecasting*, **16**, 2, 219-233.

Dunkerton, T. J., Montgomery, M. T. and Wang, Z., 2009, "Tropical cyclogenesis in a tropical wave critical layer: Easterly waves", **9**, 15, 5587-5646. https://doi.org/10.5194/acp-9-5587-2009.

Emanuel, K. A., 1986, "An air-sea interaction theory for tropical cyclones. Part I : Steady-state maintenance", *Journal of the Atmospheric Sciences*, **43**, 6, 585-605.

Emanuel, K. A., 1999, "Thermodynamic control of hurricane intensity", *Nature*, **401**, 6754, p665.

Emanuel, Kerry A. and Nolan, D. S., 2004, "Tropical cyclone activity and the global climate system", Preprints, 26thConf. on Hurricanes and Tropical Meteorology, Miami, FL, *Amer. Meteor. Soc. A*., Vol. **10**.

ERA-Interim datasets, 2019, retrieved from https://apps.ecmwf.int/ datasets/data/interim-full-daily/levtype=pl/.

Free, M., Bister, M. and Emanuel, K., 2004, "Potential intensity of tropical cyclones: Comparison of results from radiosonde and reanalysis data", *Journal of Climate*, **17**, 8, 1722-1727.

Ganesh, S. S., Abhilash, S., Sahai, A. K., Joseph, S., Chattopadhyay, R., Mandal, R., Dey, A. and Phani, R., 2019, "Genesis and track prediction of pre-monsoon cyclonic storms over North Indian Ocean in a multi-model ensemble framework", *Natural Hazards*, **95**, 3, 823-843.

Ganesh, S. S., Sahai, A. K., Abhilash, S., Joseph, S., Dey, A., Mandal, R., Chattopadhyay, R. and Phani, R., 2018, "A new approach to improve the track prediction of tropical cyclones over north Indian Ocean", *Geophysical Research Letters*, **45**, 15, 7781-7789.

Ganesh, S. S., Sahai, A. K., Abhilash, S., Joseph, S., Kaur, M. and Phani, R., 2020, "An improved cyclogenesis potential and storm evolution parameter for North Indian Ocean", *Earth and Space Science*, **7**, 10, p.e2020EA001209.

Gray, W. M., 1979, "Hurricanes: their formation, structure and likely role in the tropical circulation. Supplement of Meteorology Over the Tropical Oceans", RMS, James Glaisher House, Grenville Place, Bracknell, Berkshire, RG 12 1BX, D. B. Shaw, (ed)., 155-218.

Gray, W. M., 1984, "Atlantic seasonal hurricane frequency. Part II: Forecasting its variability", *Mon. Wea. Rev*., **112**, 1669-1683.

Gray, William M., 1968, "Global view of the origin of tropical disturbances and storms", *Monthly Weather Review*, **96**, 10, 669-700.

Gray, William M., 1975, "Tropical Cyclone Genesis in the Western North Pacific", Colorado State University, Fort Collins, Deptt. of Atmospheric Science. http://hdl.handle.net/10945/32587.

Gray, William M., 1998, "The formation of tropical cyclones", *Meteorology and atmospheric physics*, **67**, 1-4, 37-69.

India Meteorological Department Best Track Data Archive, 2020, retrieved fromhttp://www.rsmcnewdelhi.imd.gov.in/images/pdf/archive/best-track/best%20track%20ecscsuc-2020.xls.

India Meteorological Department, RSMC Bulletin, Ockhi, 2017, retrieved fromhttp://www.rsmcnewdelhi.imd.gov.in/images/pdf/archive/bulletins/2017/rockhi.pdf.

India Meteorological Department, Tropical Cyclones - Frequently Asked Questions, 2016, retrieved from http://www.rsmcnewdelhi.imd.gov.in/images/pdf/cyclone-awareness/terminology/faq.pdf

Joseph, Susmitha, Sahai A. K., Sharmila, S., Abhilash, S., Borah, N., Chattopadhyay, R., Pillai P. A., Rajeevan, M. and Kumar, Arun, 2015, "North Indian heavy rainfall event during June 2013: diagnostics and extended range prediction", *Climate Dynamics*, **44**, 2049-2065, doi:10.1007/s00382-014-2291-5, 2049-2065.

Kaur, M., Krishna, R. P. M., Joseph, S., Dey, A., Mandal, R., Chattopadhyay, R., Sahai, A. K., Mukhopadhyay, P. and Abhilash, S., 2020, "Dynamical downscaling of a multimodel ensemble prediction system : Application to tropical cyclones", *Atmospheric Science Letters*, **21**, 8. https://doi.org/10.1002/asl.971.

Kikuchi, K. and Wang, B., 2010, "Formation of tropical cyclones in the northern Indian Ocean associated with two types of tropical intraseasonal oscillation modes", *Journal of the Meteorological Society of Japan. Ser. II*, **88**, 3, 475-496.

Kotal, S. D. and Bhattacharya, S. K., 2013, "Tropical cyclone Genesis Potential Parameter (GPP) and it's application over the north Indian Sea", *MAUSAM*, **64**, 1, 149-170.

Kotal, S. D., Kundu, P. K. and Roy Bhowmik, S. K., 2009, "Analysis of cyclogenesis parameter for developing and non developing low-pressure systems over the Indian Sea", *Natural hazards*, **50**, 2, 389-402.

Krishna, K. M., 2009, "Intensifying tropical cyclones over the North Indian Ocean during summer monsoon-global warming", *Global and Planetary Change*, **65**, 1-2, 12-16.

Krishnamohan, K. S., Mohanakumar, K. and Joseph, P. V., 2012, "The influence of Madden - Julian oscillation in the genesis of north Indian Ocean tropical cyclones", *Theoretical and applied climatology*, **109**, 1-2, 271-282.

Lee, C. S., Edson, R. and Gray, W. M., 1989, "Some large-scale characteristics associated with tropical cyclone development in the North Indian Ocean during FGGE", *Monthly Weather Review*, **117**, 2, 407-426.

Li, G., Ren, B., Yang, C. and Zheng, J., 2011, "Revisiting the trend of the tropicaland subtropical Pacific surface latent heat flux during 1977-2006", *Journal of Geophys Research*, **116**. D10115. doi:10.1029/2010JD015444.

Liu, J. and Curry, J. A., 2006, "Variability of the tropical and subtropical oceansurface latent heat flux during 1989-2000", *Geophys. Res. Lett.*, **33**. L05706. doi:10.1029/2005GL024809.

McBride, John L. and Raymond Zehr, 1981, "Observational analysis of tropical cyclone formation. Part II: Comparison of non-developing versus developing systems", *Journal of the Atmospheric Sciences*, **38**, 6, 1132-1151.

Murakami, H., Vecchi, G. A. and Underwood, S., 2017, "Increasing frequency of extremely severe cyclonic storms over the Arabian Sea", *Nature : Climate Change*, **7**, 12, 885-889. DOI : https : 10.1038/s41558-017-0008-6.

Nath, Sankar, Kotal, S. D. and Kundu, P. K., 2013, "Analysis of a genesis potential parameter during pre-cyclone watch period over the Bay of Bengal", *Natural hazards*, **65**, 3, 2253-2265.

Pattanaik, D. R., Sahai, A. K., Mandal, Raju, R. Muralikrishna, Phani, Dey, Avijit, Chattopadhyay, Rajib, Joseph, Susmitha, Tiwari, Amar Deep and Mishra, Vimal, 2019, "Evolution of operational extended range forecast system of IMD : Prospects of its applications in different sectors", *MAUSAM*, **70**, 2, 233-264.

Rajasree, V. P. M., Kesarkar, A. P., Bhate, J. N., Singh, V., Umakanth, U. and Varma, T. H., 2016, "A comparative study on the genesis of North Indian Ocean tropical cyclone Madi (2013) and Atlantic Ocean tropical cyclone Florence (2006)", *Journal of Geophysical Research : Atmospheres*, **121**, 23, 13,826.

Saha, S., Moorthi, S., Wu, X., Wang, J., Nadiga, S., Tripp, P., Behringer, D., Hou, Y. T., Chuang, H. Y., Iredell, M., Ek, M., Meng, J., Yang, R., Mendez, M. P., Van Den Dool, H., Zhang, Q., Wang, W., Chen, M. and Becker, E., 2014, "TheNCEP climate forecast system version 2", *Journal of Climate*, **27**, 6, 2185-2208. https://doi.org/10.1175/JCLI-D-12-00823.1.

Sahai, A. K., Sharmila, S., Abhilash, S., Chattopadhyay, R., Borah, N., Krishna, R. P. M., Joseph, S., Roxy, M., De, S., Pattnaik, S. and Pillai, P. A., 2013, "Simulation and extended range prediction ofmonsoon intraseasonal oscillations in NCEP CFS/GFS version2 framework", *Current Science*, **104**, 10, 1394-1408

Zehr, R. M., 1992, "Tropical cyclogenesis in the western North Pacific".

Zhou, L. T., Chen, G. and Wu, R., 2015, "Change in surface latent heat flux and its association with tropical cyclone genesis in the western North Pacific", *Theor. Appl. Climatol*., **119**, 221. https://doi.org/10.1007/s00704-014-10.